THE JOURNAL OF BIOLOGICAL CHEMISTRY VOL. 287, NO. 13, pp. 10277–10288, March 23, 2012

Hepatocyte-specific Deletion of Janus Kinase 2 (JAK2) Protects against Diet-induced Steatohepatitis and Glucose Intolerance*[S]

Received for publication, October 30, 2011, and in revised form, January 18, 2012 Published, JBC Papers in Press, January 24, 2012, DOI 10.1074/jbc.M111.317453

Sally Yu Shi[‡§1,2], Rubén García Martin[‡1,3], Robin E. Duncan[¶], Diana Choi[‡§4], Shun-Yan Lu[‡], Stephanie A. Schroer[‡], Erica P. Cai[‡§5], Cynthia T. Luk[‡§6], Kathryn E. Hopperton[¶], Anthony F. Domenichiello[¶], Christine Tang[‖], Mark Naples[**], Mark J. Dekker[**], Adria Giacca[‖], Khosrow Adeli[**], Kay-Uwe Wagner[‡‡], Richard P. Bazinet[¶], and Minna Woo[‡§ §§7]

From the [‡]Toronto General Research Institute, Toronto, Ontario M5G 2C4, Canada, the [§]Institute of Medical Science, University of Toronto, Toronto, Ontario M5G 2M9, Canada., the [¶]Department of Nutritional Sciences, University of Toronto, Toronto, Ontario M5S 3E2, Canada, the [‖]Department of Physiology, Faculty of Medicine, University of Toronto, Toronto, Ontario M5S 1A8, Canada, the [**]Molecular Structure and Function, Research Institute, The Hospital for Sick Children, University of Toronto, Toronto, Ontario M5G 1X8, Canada, the [‡‡]Eppley Institute for Research in Cancer and Allied Diseases and the Department of Pathology and Microbiology, University of Nebraska Medical Center, Omaha, Nebraska 68198-6805, and the [§§]Department of Medicine and Keenan Research Centre in the Li Ka Shing Knowledge Institute, St. Michael's Hospital, Toronto, Ontario M3B 1W5, Canada

Background: JAK2 mediates signaling by a number of cytokines in the liver.
Results: Hepatic JAK2 KO mice developed spontaneous steatosis but were protected from high fat diet-induced steatohepaitits and insulin resistance.
Conclusion: Hepatic JAK2 is required for the development of diet-induced steatohepatitis and glucose intolerance.
Significance: Understanding the role of JAK2 in metabolism will provide insights into the pathogenesis of the metabolic syndrome.

Non-alcoholic fatty liver disease (NAFLD) is becoming the leading cause of chronic liver disease and is now considered to be the hepatic manifestation of the metabolic syndrome. However, the role of steatosis *per se* and the precise factors required in the progression to steatohepatitis or insulin resistance remain elusive. The JAK-STAT pathway is critical in mediating signaling of a wide variety of cytokines and growth factors. Mice with hepatocyte-specific deletion of *Janus kinase 2* (L-JAK2 KO mice) develop spontaneous steatosis as early as 2 weeks of age. In this study, we investigated the metabolic consequences of *jak2* deletion in response to diet-induced metabolic stress. To our surprise, despite the profound hepatosteatosis, deletion of hepatic *jak2* did not sensitize the liver to accelerated inflammatory injury on a prolonged high fat diet (HFD). This was accompanied by complete protection against HFD-induced whole-body insulin resistance and glucose intolerance. Improved glucose-stimulated insulin secretion and an increase in β-cell mass were also present in these mice. Moreover, L-JAK2 KO mice had progressively reduced adiposity in association with blunted hepatic growth hormone signaling. These mice also exhibited increased resting energy expenditure on both chow and high fat diet. In conclusion, our findings indicate a key role of hepatic JAK2 in metabolism such that its absence completely arrests steatohepatitis development and confers protection against diet-induced systemic insulin resistance and glucose intolerance.

Nonalcoholic fatty liver disease (NAFLD)[8] is increasingly recognized as the leading cause of chronic liver disease, affecting about 20–30% of the population in Western countries (1, 2). Because of its strong link with insulin resistance and type 2 diabetes, NAFLD is now considered to be the hepatic manifestation of the metabolic syndrome (3). NAFLD comprises a spectrum, where steatosis alone is largely benign but can progress to steatohepatitis characterized by inflammation and fibrosis, followed by cirrhosis, liver failure, and in some cases hepatocellular carcinoma (4, 5). The exact pathogenesis of

* This work was supported by operating grants from Canadian Institute of Health Research MOP-191501 and Canadian Diabetes Association (to M. W.).
[S] This article contains supplemental Figs. S1–S3.
[1] Both authors contributed equally to this work.
[2] Supported by the Banting and Best Diabetes Centre (BBDC)-Novo Nordisk Studentship and the NSERC Alexander Graham Bell Canada Graduate Scholarship.
[3] Supported by the Spanish National Research Fellowship from Ibercaja Foundation (Spain).
[4] Supported by the CIHR Federick Banting and Charles Best Canada Graduate Scholarship - Doctoral.
[5] Supported by the Canadian Diabetes Association Doctoral Student Research Award.
[6] Supported by the Eliot Phillipson Clinician Scientist Training Program and the BBDC post-doctoral fellowship.
[7] To whom correspondence should be addressed: MaRS Centre, Toronto Medical Discovery Tower, 101 College Street, 10th floor, Room 10-361, Toronto, ON M5G 1L7 Canada. Tel.: 416-581-7531; Fax: 416-581-7880; E-mail: mwoo@uhnres.utoronto.ca.

[8] The abbreviations used are: NAFLD, non-alcoholic fatty liver disease; TG, triglyceride; JAK, Janus kinase; STAT, signal transducer and activator of transcription; GH, growth hormone; IGF-1, insulin-like growth factor 1; HFD, high fat diet; GTT, glucose tolerance test; ITT, insulin tolerance test; ALT, alanine aminotransferase; AST, aspartate aminotransferase; FFA, free fatty acid; RER, respiratory exchange ratio; KO, knockout; DAG, diacylglycerol.

NAFLD, however, is not well understood. Insulin resistance is known to play a critical role in lipid overaccumulation in the liver. The resulting steatosis can in turn further impair insulin signaling and sensitize the liver to inflammatory injury induced by a variety of stimuli (6). However, accumulating data now indicate that hepatic overstorage of triglyceride (TG) *per se* is not a requirement for deterioration of insulin signaling and progression of inflammation and may even be protective against lipotoxicity (7–10). Nonetheless, the role of steatosis *per se* in the development of insulin resistance and diabetes remains elusive.

The Janus kinase-signal transducers and activators of transcription (JAK-STAT) pathway is one of the major inflammatory pathways signaling downstream of cytokines. In the liver, JAK2 is activated by several cytokines and growth factors including IFN-γ, IL-4, IL-6, IL-12, IL-13, growth hormone (GH), and leptin (11). Disruption of hepatic leptin signaling promoted intrahepatic lipid accumulation but protected from diet- and age-induced glucose intolerance (12). On the other hand, hepatic STAT3 inactivation up-regulated expression of gluconeogenic and lipogenic genes, leading to both hepatic and systemic insulin resistance and TG accumulation (13). GH, which signals through the GH receptor to activate the JAK2-STAT5 pathway, antagonizes insulin action by raising blood glucose levels, reducing peripheral insulin sensitivity and stimulating lipolysis of the adipose tissue (14). Mice with hepatic deletion of the GH receptor, STAT5 and IGF-1 all developed insulin resistance and glucose intolerance (15–17). This phenotype was proposed to be secondary to elevated serum GH levels resulting from loss of feedback inhibition by IGF-1. In addition, both hepatic GH receptor- and STAT5-deficient mice exhibited marked steatosis (15, 16, 18). Recently, it was shown that deletion of *jak2* in hepatocytes led to spontaneous steatosis, and this was dependent on excess GH signaling such that abolishment of aberrant GH secretion completely rescued the fatty liver phenotype (19).

In this study, we sought to invesigate the metabolic and inflammatory consequences of hepatic *jak2* deletion in response to metabolic stress. To determine the role of hepatic JAK2 in diet-induced insulin resistance, we fed a cohort of L-JAK2 KO mice and their littermate controls a high fat diet (HFD). HFD feeding for a prolonged period of time induces a chronic inflammatory state that is thought to underlie the accompanying metabolic abnormalities including insulin resistance and hepatocellular damage (20). Surprisingly, the profound hepatosteatosis seen in L-JAK2 KO mice did not predispose to development of HFD-induced steatohepatitis; and despite impaired signal transduction through Akt in the liver, improved insulin signaling in the adipose tissue and protection against systemic insulin resistance were observed in L-JAK2 KO mice. Moreover, L-JAK2 KO mice were completely protected against development of diet-induced glucose intolerance. This metabolically beneficial profile may be accounted for, at least in part, by compensatory β cell proliferation and enhanced glucose-stimulated insulin secretion.

EXPERIMENTAL PROCEDURES

Generation of L-JAK2 KO Mice—Mice with hepatocyte-specific JAK2 deficiency were generated by breeding mice with the *jak2* gene flanked by loxP sites ($jak2^{fl/fl}$) (21) to mice that harbored the *cre* transgene under control of the albumin promoter obtained from the Jackson Laboratory ($AlbCre^{+}$). The resulting $AlbCre^{+}$ $jak2^{+/fl}$ mice were intercrossed to generate $AlbCre^{+}$ $jak2^{fl/fl}$ (L-JAK2 KO) and $AlbCre^{+}$ $jak2^{+/+}$ (Control) mice. Mice used in this study were maintained on a mixed C57BL/6 and C3H/HeJ background. Both male and female mice were used. The efficient deletion of *jak2* in hepatocytes was confirmed by immunoblotting (supplemental Fig. S1). Animals were maintained on a 12:12-hr light-dark cycle with free access to water and standard irradiated rodent chow (5% fat; Harlan Teklad) and housed in a pathogen-free barrier facility at the Ontario Cancer Institute (Toronto, ON, Canada). Some mice were fed a HFD (60% fat, 24% carbohydrates and 16% protein based on caloric content; F3282; Bio-Serv) for 8–10 weeks starting at 2 months of age. All animal experiments were approved by the Ontario Cancer Institute Animal Care Facility.

In Vivo Metabolic Analyses—All overnight fasts were carried out between 5:00 PM and 9:00 AM. Blood glucose measurements, glucose tolerance test (GTT), insulin tolerance test (ITT), and glucose-stimulated insulin secretion were performed as previously described (22). For insulin signaling experiments, mice fasted overnight were injected intraperitoneal with human regular insulin (5 units/kg, Humulin R, Lilly) or PBS. Tissues were harvested 10 min later and snap frozen in liquid nitrogen. Rectal temperature was measured in randomly fed mice at 10:00 AM. To measure energy expenditure, mice were individually housed in metabolic cages with free access to food and water. After 24 h acclimation to the apparatus, data for 24-h measurement were collected and analyzed using a comprehensive lab animal monitoring system (Columbus Instruments). Food consumption was determined by weighing the chow before and after the measurement and normalized to body weight.

Hyperinsulinemic-Euglycemic Clamp—Hyperinsulinemic-euglycemic clamp was performed as previously described (23). Briefly, following a 5-h fast, [3-^{3}H]glucose (Perkin-Elmer) infusion (2.8 μCi bolus, 0.052 μCi/min) was initiated for a 120-min equilibration period. During the last 30 min, three sequential blood samples were taken at 10-min intervals for determination of glucose-specific activity. At time 0, a continuous infusion of human insulin (Humulin R; 5mU/kg/min) was initiated. Blood glucose was measured every 10 min and a 30% glucose solution was infused at a variable rate to maintain euglycemia. Steady state was achieved when the glucose infusion rate to maintain blood glucose was constant for 30 min.

Analysis of Serum Parameters—Overnight fasted mice were anesthetized and blood was collected by cardiac puncture. Serum alanine aminotransferase (ALT) and aspartate aminotransferase (AST) levels were measured by IDEXX Ltd. (Markham, Ontario, Canada). Insulin levels were measured by a mouse insulin ELISA kit (Crystal Chem Inc.). Serum leptin, GH, and IGF-1 levels were determined by radioimmunoassay, serum-free fatty acids (FFA) were determined using the hep-

tane/isopropanol extraction method, and serum adiponectin, TNF-α and IL-6 levels were determined by the Luminex100 System at the Mouse Metabolic Phenotyping Centre (Vanderbilt University, Nashville, TN).

Hepatic Lipid Content and FA Composition—Total liver TG and cholesterol content was extracted in chloroform/methanol (2:1, v/v) and measured using commercially available kits (Randox). Fatty acid composition of hepatic lipid esters was analyzed as previously described (24). Ceramide content was analyzed by liquid chromatography tandem mass spectrometry (LC/MS/MS) as previously described (25).

Histology, Immunohistochemistry, and Immunofluorescence—Liver and pancreatic tissues were harvested after an overnight fast and fixed in 4% paraformaldehyde in 0.1 M PBS (pH 7.4). Liver sections were stained with hematoxylin-eosin and Masson's trichrome stain. Immunofluorescent staining was performed with anti-F4/80 antibody (Santa Cruz Biotechnology) and visualized using a Zeiss inverted fluorescent microscope. Immunohistochemistry was performed on pancreatic sections using anti-insulin antibody (Dako). Scanned sections were analyzed with ImageScope version 11.0.2.716 software (Aperio Technologies).

Immunoblotting—Protein lysates were subjected to immunoblotting as previously described (22). The following antibodies were used: phospho-JAK2 (Tyr1007/8); phospho-STAT3 (Tyr705); total STAT3; total STAT5; phospho-Akt (Ser473), total Akt; GAPDH (Cell Signaling Technology); phospho-STAT5 (Tyr694) (Zymed Laboratories Inc.); and total JAK2 (Upstate). Band intensities were quantified using ImageJ software.

Quantitative RT-PCR—Total RNA from liver tissues was isolated with RNeasy Mini Kit (Qiagen) according to manufacturer's protocol. RNA was reverse-transcribed with random primers using M-MLV enzyme (Invitrogen), and real-time PCR was performed using SYBR Green master mix (Applied Biosystems) on a 7900HT Fast-Real Time PCR System (Applied Biosystem). Each sample was run in triplicate. Primer sequences are available upon request.

Statistical Analysis—Data are presented as means ± S.E. Values were analyzed by Student's *t* test, using GraphPad Prism version 5. p values < 0.05 were accepted as statistically significant.

RESULTS

L-JAK2 KO Mice Develop Progressive Hepatic Steatosis—L-JAK2 KO mice developed striking hepatic steatosis spontaneously on chow diet, which was grossly visible by the pale and glistening appearance of the liver at 2–3 months of age (Fig. 1*A*). Their liver weight expressed as a percentage of total body weight was significantly higher than control littermates (Fig. 1*B*). Using Oil-red-O staining, we observed intrahepatic lipid accumulation by as early as 2 weeks of age (Fig. 1*C*). TG was the predominant lipid species accounting for steatosis, which progressively accumulated with age (Fig. 1*D*). Analysis of the profile of fatty acids (FA) esterified to TG indicated elevated levels of all the long-chain saturated and monounsaturated FA in livers from L-JAK2 KO mice (Fig. 1*E*). We next analyzed for the presence of bioactive lipid metabolites implicated in insulin resistance. Hepatic cholesterol levels were not significantly different between L-JAK2 KO mice and control littermates (Fig. 1*F*). Diacylglycerol (DAG) content was increased by about 50% in livers of L-JAK2 KO mice compared with control littermates at 6 months of age (Fig. 1*G*). Hepatic levels of ceramide, total FFA and free palmitate, however, were similar between the two groups (Fig. 1, *H–J*).

L-JAK2 KO Mice Do Not Progress to Steatohepatitis on a HFD—According to the "two-hit" model proposed by Day and James (6), steatosis sensitizes the liver to inflammatory injury. To examine whether the profound steatosis seen in L-JAK2 KO mice predisposes to development of steatohepatitis, we fed the knock-out mice and their littermate controls a HFD for 8–10 weeks starting at 2 months of age. As expected, control mice developed hepatic steatosis after prolonged HFD feeding, and this was further exacerbated by abolishment of hepatic JAK2 signaling (Fig. 2*A*). Interestingly, histological analysis of liver sections using Masson's trichrome stain indicated that L-JAK2 KO mice did not exhibit increased inflammatory injury or fibrogenesis (Fig. 2*B*). This lack in progression of inflammation persisted up to 11 months of age in chow-fed L-JAK2 KO mice (Fig. 2*C*). There was also no significant increase in macrophage accumulation in livers of knock-out mice as shown by immunofluorescence staining and quantitative RT-PCR (Fig. 2, *D* and *E*). Serum levels of ALT, reflective of the degree of hepatic steatosis, trended higher in chow-fed L-JAK2 KO mice. On the other hand, despite the profound steatosis, circulating levels of AST, a hallmark of hepatocyte injury, was not elevated under both chow- and HFD-fed conditions (Fig. 2*F*). Circulating levels of total bilirubin and albumin were similar (supplemental Fig. S2*A* and *B*), suggesting that livers of L-JAK2 KO mice were able to maintain their synthetic and secretory capacity. Furthermore, genes encoding inflammatory cytokines including TNF-α, IL-1β, and IFN-γ were not up-regulated in HFD-fed L-JAK2 KO mice (Fig. 2*G*). In fact, hepatic expression of an inflammatory cytokine, IL-6, was significantly lower. We also measured circulating levels of TNF-α and IL-6 and found no significant difference in levels of either cytokine between L-JAK2 KO mice and littermate controls under either chow- or HFD-fed conditions (Fig. 2*H*).

L-JAK2 KO Mice Display Impaired Hepatic Insulin Signaling but Normal Systemic Insulin Sensitivity—Fatty liver is commonly associated with insulin resistance and type 2 diabetes; therefore, we examined the impact of hepatocyte-specific *jak2* deletion on both hepatic and systemic insulin signaling. Fasting serum insulin levels were not significantly different between the two genotypes on either chow or HFD (Fig. 3*A*), suggesting absence of whole-body insulin resistance. Moreover, despite the profound hepatosteatosis in HFD-fed L-JAK2 KO mice, they did not display whole body insulin resistance as evidenced by similar glucose lowering by exogenous insulin by intraperitoneal insulin tolerance test (Fig. 3*B*). Next, to specifically examine insulin sensitivity in individual metabolic tissues, L-JAK2 KO mice and littermate controls were injected with insulin intraperitoneal, and tissues were harvested 10 min later for analysis of insulin signaling by Western blotting. As shown in Fig. 3*C*, Akt phosphorylation was significantly attenuated in the livers of L-JAK2 KO mice following insulin stimulation, whereas in adipose tissue (Fig. 3*C*) and skeletal muscle (data not

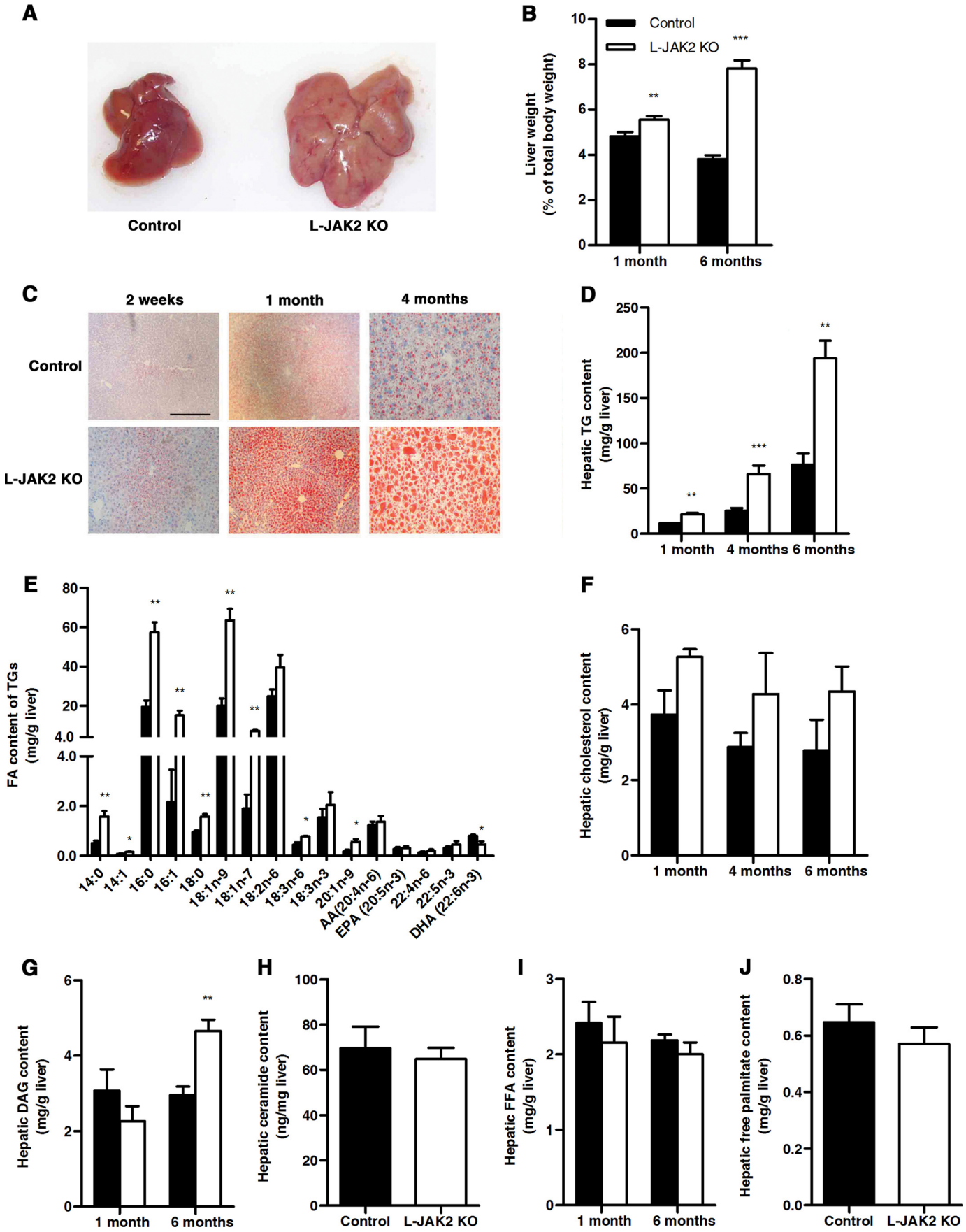
A
Control
L-JAK2 KO
B
Control
L-JAK2 KO
Liver weight (% of total body weight)
1 month
6 months
C
2 weeks
1 month
4 months
Control
L-JAK2 KO
D
Hepatic TG content (mg/g liver)
1 month
4 months
6 months
E
FA content of TGs (mg/g liver)
14:0
14:1
16:0
16:1
18:0
18:1n-9
18:1n-7
18:2n-6
18:3n-6
18:3n-3
20:1n-9
AA(20:4n-6)
EPA (20:5n-3)
22:4n-6
22:5n-3
DHA (22:6n-3)
F
Hepatic cholesterol content (mg/g liver)
1 month
4 months
6 months
G
Hepatic DAG content (mg/g liver)
1 month
6 months
H
Hepatic ceramide content (ng/mg liver)
Control
L-JAK2 KO
I
Hepatic FFA content (mg/g liver)
1 month
6 months
J
Hepatic free palmitate content (mg/g liver)
Control
L-JAK2 KO

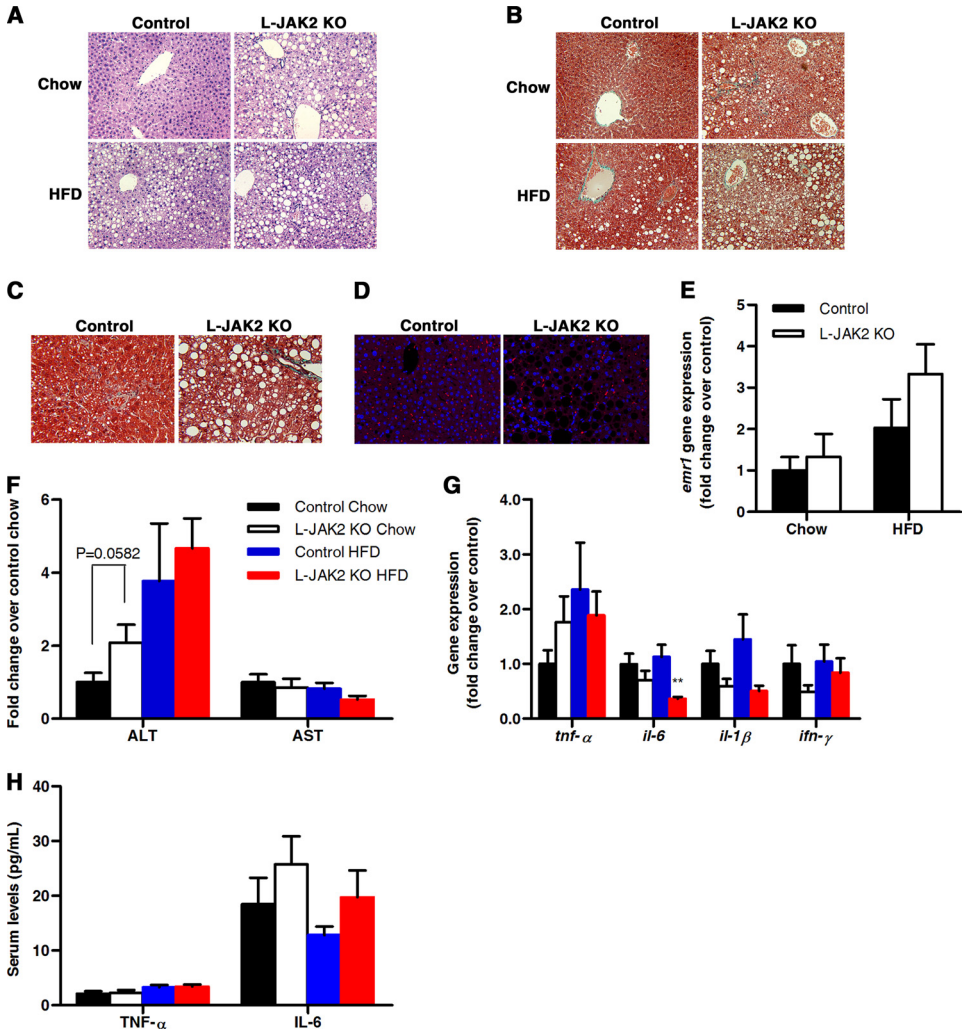

FIGURE 2. **No progression to steatohepatitis on a HFD in L-JAK2 KO mice.** *A* and *B*, representative photographs of (*A*) hematoxylin and eosin, and (*B*) Masson's trichrome staining of liver sections from 4-month-old L-JAK2 KO mice and control littermates after 8–10 weeks on a standard chow or HFD (original magnification ×25). *C*, representative photographs of Masson's trichrome staining of liver sections from 11-month-old chow-fed mice (original magnification ×25). *D*, immunofluorescent staining of macrophages (in *red*) in livers from 4-month-old chow-fed mice using anti-F4/80 antibody (original magnification ×20). *E*, quantitative RT-PCR analysis of mRNA expression of *emr1* (F4/80) in livers from chow- and HFD-fed mice ($n \geq 5$ per group). Values are normalized to 18S mRNA levels and expressed as fold changes relative to the chow control group. *F*, serum levels of ALT and AST in chow- and HFD-fed mice ($n \geq 5$ per group). Values are expressed as fold change over the chow control group. *G*, mRNA expression of genes encoding inflammatory markers in livers from chow- and HFD-fed mice ($n \geq 8$ per group). Values are normalized to 18S mRNA levels and expressed as fold changes relative to the chow control group. *tnf-α*, tumor necrosis factor α; *il-6*, interleukin-6; *il-1β*, interleukin-1β; *ifn-γ*, interferon γ. *H*, serum levels of TNF-α and IL-6 in chow- and HFD-fed mice ($n \geq 5$ per group). Results are mean ± S.E. *, $p < 0.05$ *versus* control littermates.

shown) this attenuation in insulin response was not present compared with littermate controls. Consistent with attenuated insulin signaling in the liver, hyperinsulinemic-euglycemic clamp studies showed impaired suppression of endogenous glucose production by insulin in L-JAK2 KO mice. On the other hand, insulin-induced whole-body glucose utilization was comparable between the two genotypes, in accordance with absence of systemic insulin resistance in L-JAK2 KO mice (Fig. 3*D*). To assess for potential changes in hepatic gluconeogenic program, we measured hepatic expression of key gluconeogenic enzymes including PEPCK and G6Pase in overnight fasted mice and found no significant difference between L-JAK2 KO mice and control littermates.

L-JAK2 KO Mice Are Protected from Diet-induced Glucose Intolerance—In agreement with normal peripheral glucose disposal but dysregulated hepatic glucose production, fasting (Fig.

FIGURE 1. **Progressive hepatic steatosis in L-JAK2 KO mice.** *A*, representative photographs of liver lobes harvested from 12-week-old mice. *B*, liver weight normalized to total body weight in L-JAK2 KO mice and littermate controls ($n \geq 6$ per group). *C*, representative photographs of Oil-Red-O staining of liver sections from mice at 2 weeks, 1 month, and 4 months of age after 16 h of fasting. Scale bar: 200 μm. *D*, hepatic TG content at 1, 4, and 6 months of age. Results are normalized to tissue weight. ($n = 3–8$ per group). *E*, extracted TG from livers of 6-month-old mice was converted to FA methyl esters and fatty acid composition was analyzed with a gas chromatography system ($n = 3–4$ per group). *AA*: arachidonic acid; *EPA*: eicosapentaenoic acid; *DHA*: docosahexaenoic acid. *F*, hepatic cholesterol content at 1, 4, and 6 months of age, represented as mg total cholesterol per gram of liver tissue ($n = 3–6$ per group). *G*, hepatic DAG content at 1 ($n = 8$) and 6 ($n = 4$) months of age. *H*, hepatic ceramide content at 1 month of age ($n = 7$). *I*, hepatic total FFA content at 1 ($n = 8$) and 6 ($n = 4$) months of age. *J*, hepatic free palmitate content at 1 month of age ($n = 5$ per group), normalized to liver tissue weight. Results are mean ± S.E. *, $p < 0.05$; **, $p < 0.01$; ***, $p < 0.001$.

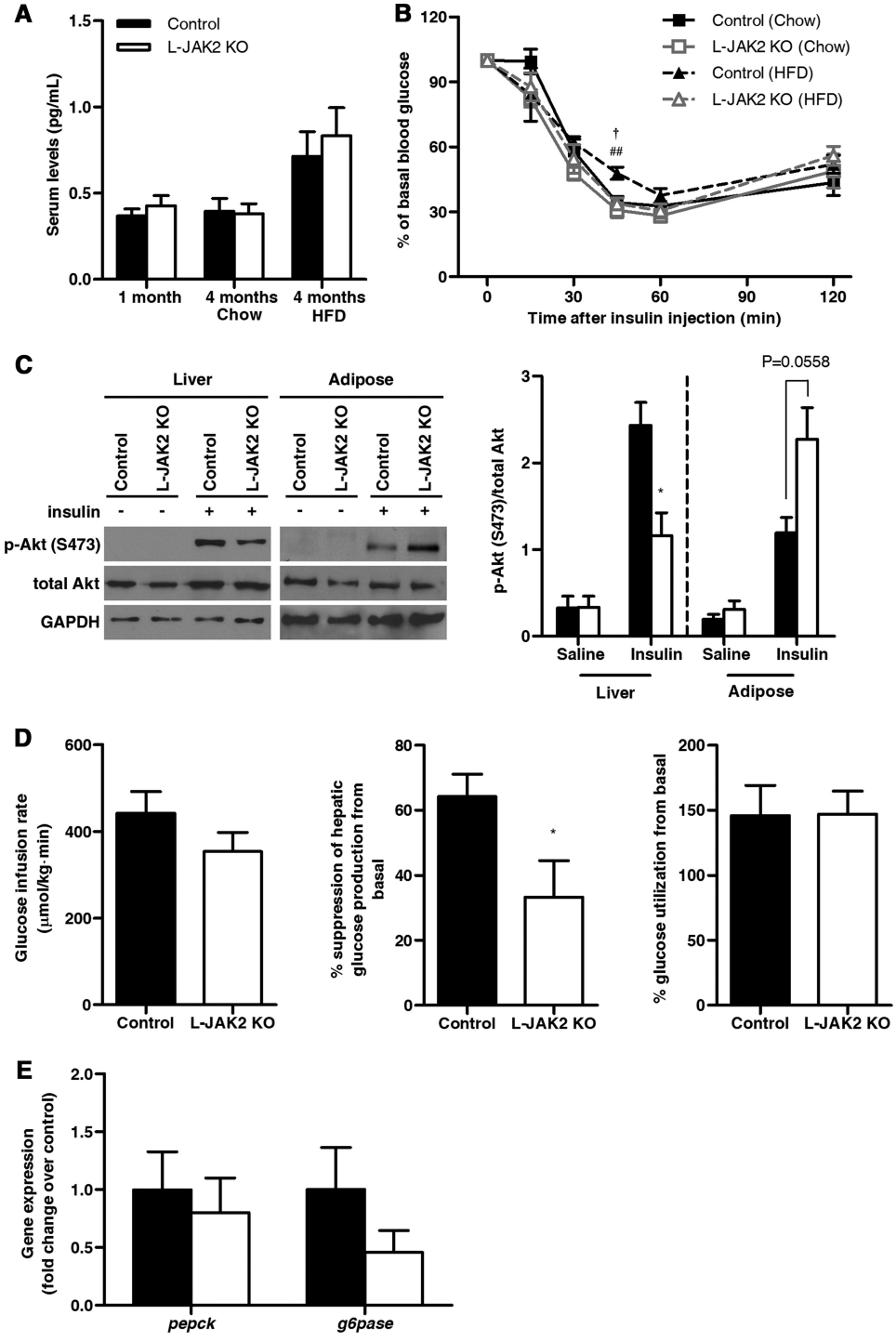

FIGURE 3. **Attenuated hepatic insulin sensitivity but normal systemic insulin sensitivity in L-JAK2 KO mice.** *A*, fasting serum insulin levels. *B*, results of intraperitoneal insulin (1.5 units/kg) tolerance test in chow- and HFD-fed mice ($n \geq 5$ per group). ##, $p < 0.01$ Control HFD *versus* L-JAK2 KO HFD; and †, $p < 0.05$ Control Chow *versus* Control HFD. *C*, liver and subcutaneous fat lysates were prepared from L-JAK2 KO mice and control littermates 10 min after an intraperitoneal injection of insulin (5 units/kg) or saline and resolved by SDS-PAGE. Lysates were immunoblotted with anti-phospho-Akt (S473), total Akt, or anti-GAPDH antibodies. Protein band intensity was quantified by ImageJ software, and expression level of p-Akt is normalized to that of total Akt ($n = 3$ per group). *D*, steady-state glucose infusion rate, suppression of hepatic glucose production and glucose utilization measured during hyperinsulinemic-euglycemic clamps in 4-month-old chow-fed mice ($n = 5$ per group). *E*, mRNA expression of gluconeogenic genes, *pepck* and *g6pase* ($n = 7$ per group), in livers from overnight fasted L-JAK2 KO mice and littermate controls. Values are normalized to *18s* mRNA levels and expressed as fold changes relative to control. *Pepck*, phosphoenolpyruvate carboxykinase; *g6pase*, glucose-6-phosphatase. Results are mean ± S.E. *, $p < 0.05$.

4*A*), but not random (Fig. 4*B*) blood glucose was consistently elevated in L-JAK2 KO mice compared with littermate controls. Surprisingly, L-JAK2 KO mice were found to be more glucose tolerant than littermate controls on a chow diet. This difference was more pronounced on a HFD such that l-JAK2 KO mice were completely protected against HFD-induced glu-

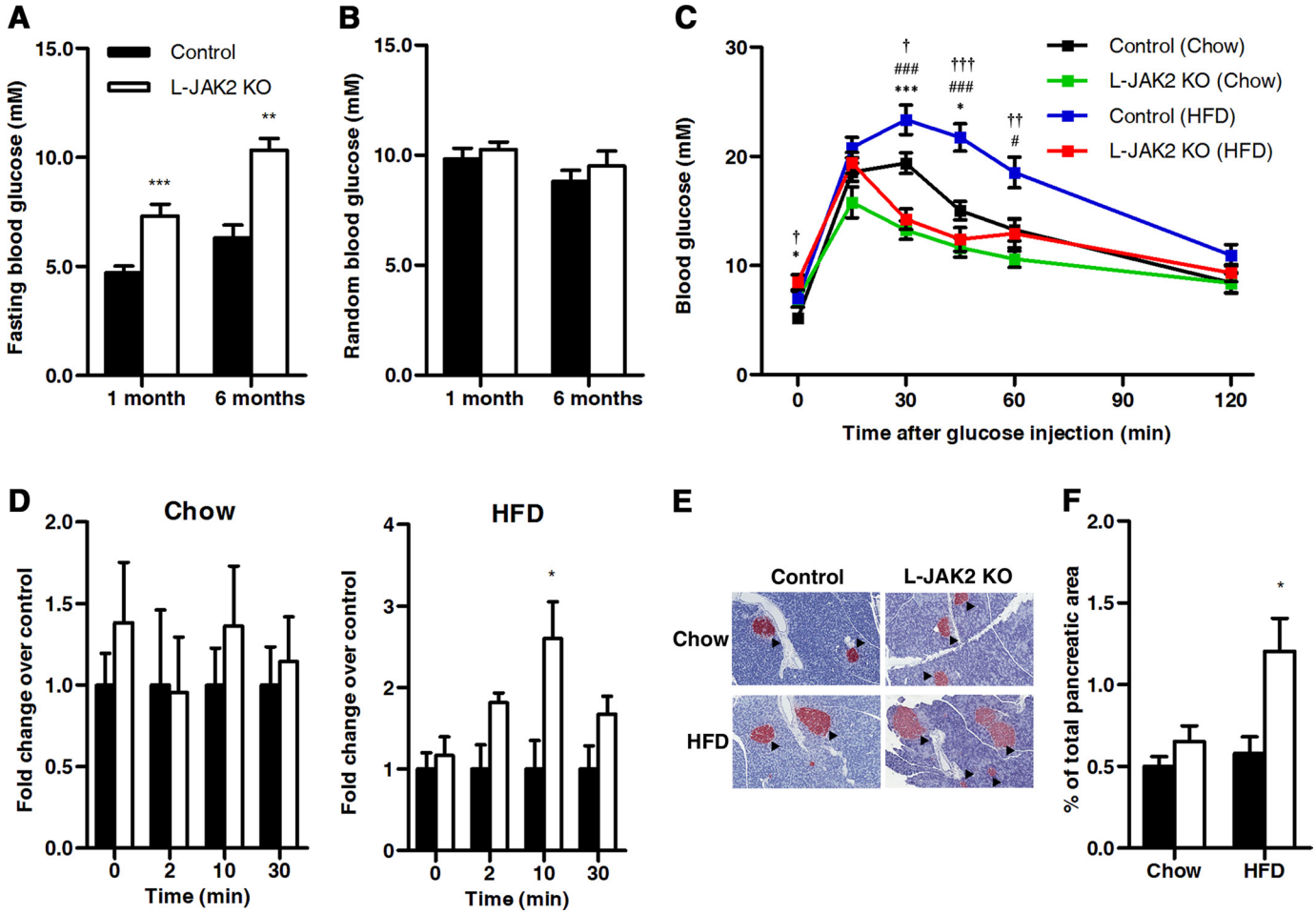

FIGURE 4. **L-JAK2 KO mice are protected from glucose intolerance.** *A*, fasting and *B*, random blood glucose at 1 ($n = 17–21$) and 6 ($n = 4–8$) months of age. *C*, results of intraperitoneal glucose (1 g/kg) tolerance test ($n \geq 8$). *, $p < 0.05$; ***, $p < 0.001$ Control Chow *versus* L-JAK2 KO Chow; #, $p < 0.05$; ###, $p < 0.001$ Control HFD *versus* L-JAK2 KO HFD; and †, $p < 0.05$; ††, $p < 0.01$; †††, $p < 0.001$ Control Chow *versus* Control HFD. *D*, serum insulin levels in response to an intraperitoneal injection of 3 g/kg glucose. Values are expressed as fold change over the control group ($n \geq 5$). *E*, representative photographs of pancreatic sections stained with anti-insulin antibody (original magnification ×10). *Arrowheads* point to pancreatic islets. *F*, quantification of β-cell area from pancreatic sections stained for insulin in *E*, expressed as percent of total pancreatic area ($n \geq 7$). Results are mean ± S.E. *, $p < 0.05$; **, $p < 0.01$; ***, $p < 0.001$.

cose intolerance (Fig. 4*C*). To delineate potential mechanisms underlying the improved glucose tolerance, we measured serum insulin levels in response to glucose stimulation. As shown in Fig. 4*D*, no significant difference existed between L-JAK2 KO mice and littermate controls on a chow diet. On the other hand, HFD-fed L-JAK2 KO mice secreted more insulin in response to glucose challenge. This was associated with a significantly increased β cell area in L-JAK2 KO mice on a HFD (Fig. 4, *E* and *F*). Together, these data suggest that despite the profound hepatosteatosis and dysregulated hepatic glucose production, L-JAK2 KO mice exhibit improved glucose homeostasis, which may be accounted for, at least in part, by increased insulin secretion from an enhanced β cell mass.

L-JAK2 KO Mice Exhibit Impaired Hepatic GH Signaling—In the liver, binding of GH to its receptor activates JAK2, which phosphorylates STAT5A and B, leading to transcriptional activation of a host of target genes including insulin-like growth factor 1 (*igf-1*) and suppressor of cytokine signaling 3 (*socs-3*). Similar to the findings by Sos *et al.* (19), L-JAK2 KO mice had lower serum IGF-1 levels (Fig. 5*A*) but higher serum GH levels (Fig. 5*B*), likely as a result of a release of feedback inhibition in the hypothalamus. In agreement with impaired hepatic GH signaling, phosphorylation of STAT5 was moderately reduced in livers from L-JAK2 KO mice (Fig. 5*C*). As expected, expression levels of STAT5 target genes were also decreased (Fig. 5*D*). Interestingly, phosphorylation of STAT3, another signaling partner of JAK2 that responds to cytokines such as leptin and IL-6, was increased (Fig. 5*C*). Together, these data demonstrate that JAK2 is an essential mediator of GH signaling within the liver.

L-JAK2 KO Mice Display a Reduction in Adiposity and an Increase in Energy Expenditure—Given the pivotal role of GH in metabolism, we next investigated whether hepatic JAK2 deficiency affects energy homeostasis. L-JAK2 KO mice weighed significantly less and were smaller in length compared with their control littermates by as early as one month of age, with no appreciable differences in body mass index (Fig. 6*A*). In keeping with the established effect of GH on lipolysis, L-JAK2 KO mice had decreased subcutaneous and visceral fat depot mass, which was not apparent at 1 month of age but became statistically significant at 6 months (Fig. 6*B*). In line with absence of systemic insulin resistance, circulating levels of total FFA as well as individual fatty acid species were not increased in L-JAK2 KO mice despite the reduction in adipose tissue mass (Fig. 5, *C* and

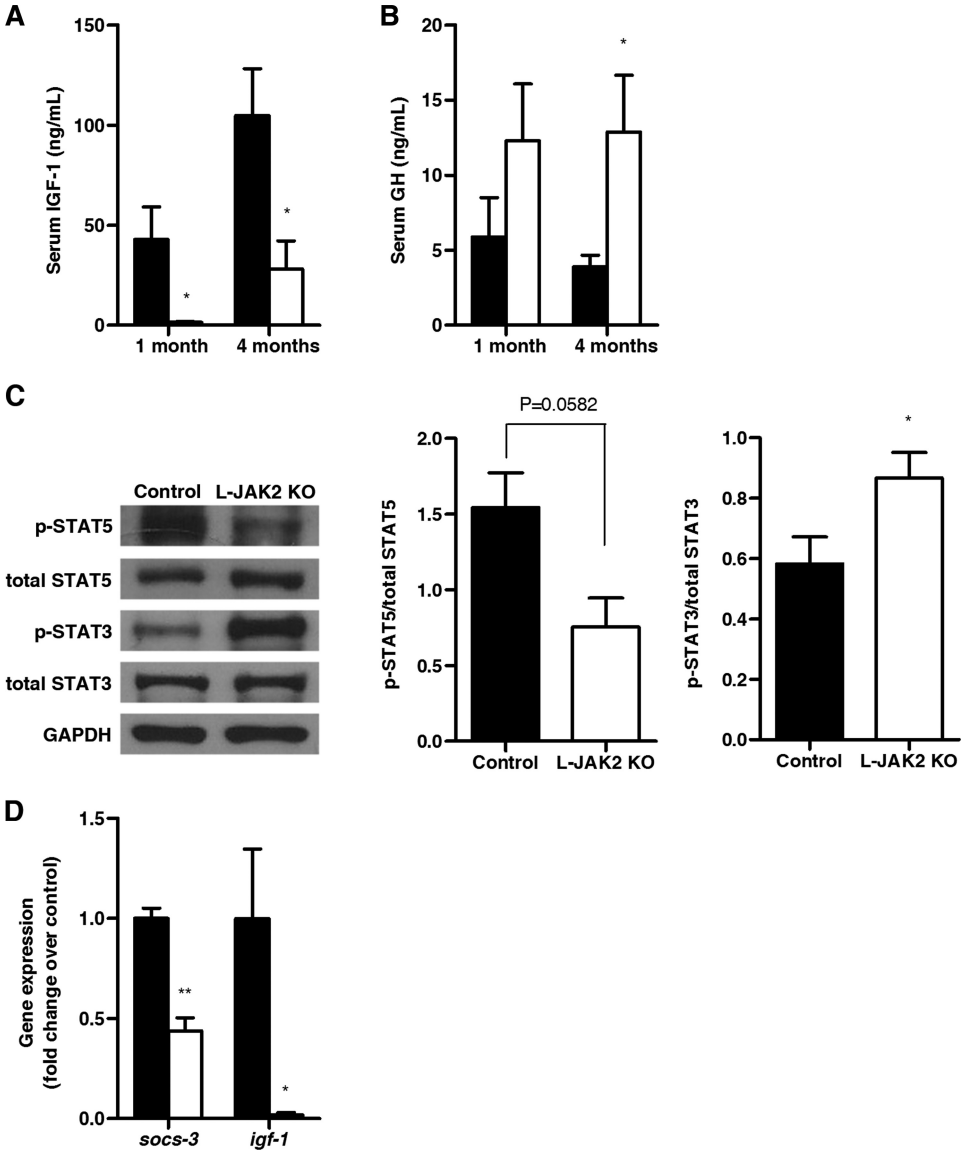

FIGURE 5. **L-JAK2 KO mice exhibit impaired hepatic GH signaling.** *A* and *B*, serum levels of (*A*) insulin-like growth factor 1 (IGF-1) and (*B*) GH measured at 1 and 4 months of age ($n \geq 5$ per group). *C*, liver lysates were prepared from 1-month-old L-JAK2 KO mice and littermate controls and resolved by SDS-PAGE. Lysates were immunoblotted with anti-phospho-STAT5, total STAT5, phospho-STAT3, total STAT3, or anti-GAPDH antibodies. Protein band intensity was quantified by ImageJ software, and levels of p-STAT5 ($n = 3$) and p-STAT3 ($n = 7$) are normalized to expression of total STAT5 and STAT3, respectively. *D*, mRNA expression of two STAT5-target genes, *socs-3* ($n = 3$) and *igf-1* ($n \geq 6$ per group), in livers from L-JAK2 KO mice and littermate controls at 1 month of age. Values are normalized to 18S mRNA levels and expressed as fold changes relative to control. *Socs-3*, suppressor of cytokine signaling 3; *igf-1*, insulin-like growth factor 1. Results are mean ± S.E. *, $p < 0.05$; **, $p < 0.01$.

D). Next, we assessed the impact of reduced fat mass on circulating levels of adipokines. Serum adiponectin levels were not significantly different between wild-type and knock-out mice (Fig. 6*E*). On the other hand, L-JAK2 KO mice had higher circulating leptin levels at 1 month of age (Fig. 6*F*) when there was no change in adiposity. As the mice aged, with diminishing fat depot mass, this difference in leptin levels was lost.

To assess energy balance in L-JAK2 KO mice, we placed them individually in metabolic chambers. Compared with their littermate controls, L-JAK2 KO mice ingested more food relative to their body weight on a chow diet (Fig. 6*G*). Furthermore, L-JAK2 KO mice exhibited a significantly greater respiratory exchange ratio (RER), indicating the preferential oxidation of glucose as the fuel source (Fig. 6*H*). Rates of O_2 consumption and CO_2 production were higher in L-JAK2 KO mice, consistent with greater energy expenditure (Fig. 6*I*). This increase in energy expenditure was also observed in HFD-fed L-JAK2 KO mice (data not shown). Locomotor activity was similar between the genotype groups (Fig. 6*J*), whereas L-JAK2 KO mice had a slightly but significantly elevated body temperature (Fig. 6*K*), indicating greater resting energy expenditure. Taken together, these results suggest that increased energy expenditure may contribute to the improved metabolic profile of L-JAK2 KO mice.

DISCUSSION

In this study, we investigated the role of hepatic JAK2, a key mediator of cytokine signaling, in diet-induced insulin resistance and glucose intolerance. By feeding L-JAK2 KO mice and their control littermates a prolonged HFD, we show that dele-

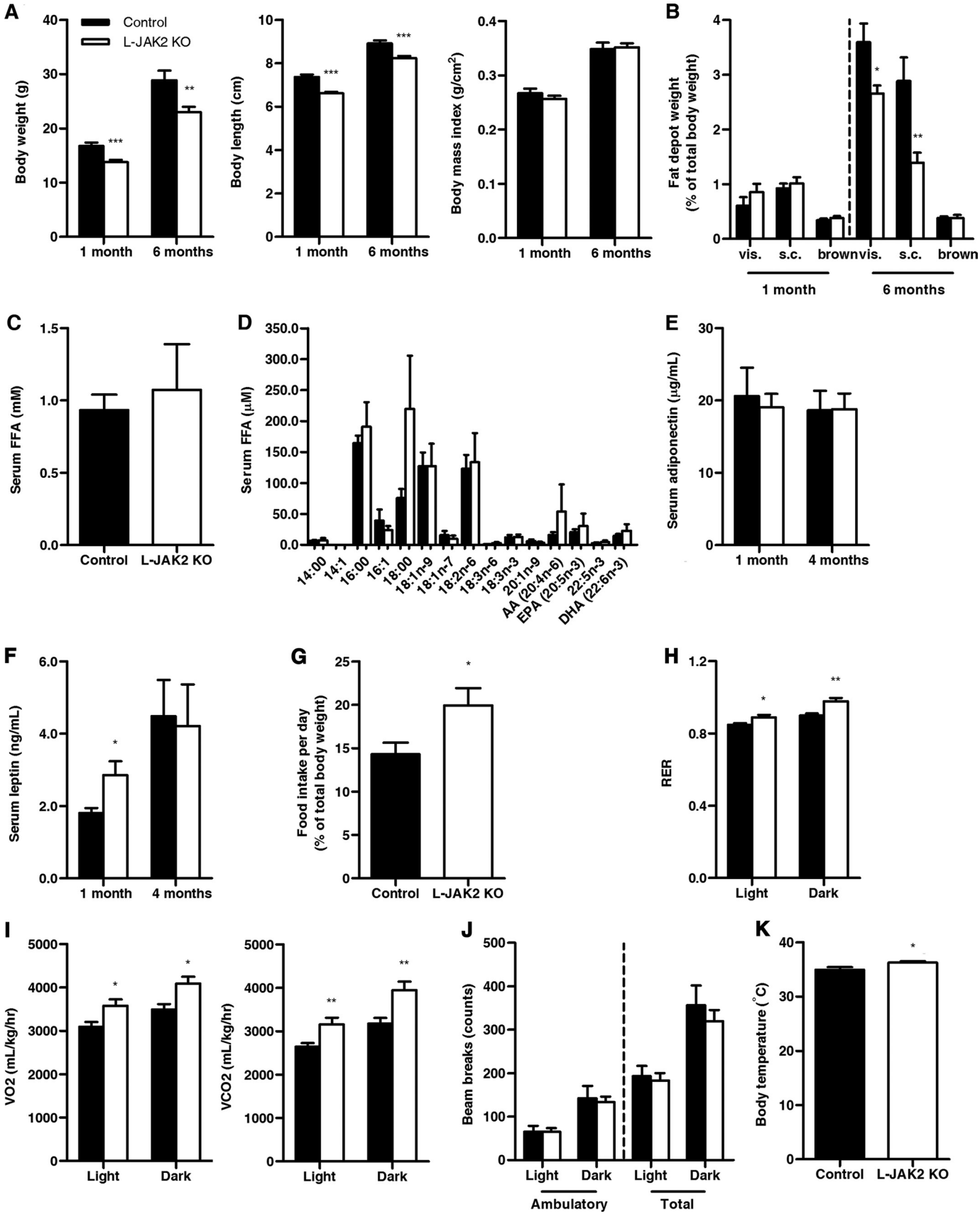
A
Control
L-JAK2 KO
Body weight (g)
1 month
6 months
Body length (cm)
Body mass index (g/cm²)
B
Fat depot weight (% of total body weight)
vis.
s.c.
brown
1 month
6 months
C
Serum FFA (mM)
Control
L-JAK2 KO
D
Serum FFA (μM)
14:00
14:1
16:00
16:1
18:00
18:1n-9
18:1n-7
18:2n-6
18:3n-6
18:3n-3
20:1n-9
AA (20:4n-6)
EPA (20:5n-3)
22:5n-3
DHA (22:6n-3)
E
Serum adiponectin (μg/mL)
1 month
4 months
F
Serum leptin (ng/mL)
1 month
4 months
G
Food intake per day (% of total body weight)
Control
L-JAK2 KO
H
RER
Light
Dark
I
VO2 (mL/kg/hr)
VCO2 (mL/kg/hr)
Light
Dark
J
Beam breaks (counts)
Light
Dark
Ambulatory
Total
K
Body temperature (°C)
Control
L-JAK2 KO

tion of hepatic *jak2* did not predispose to development of steatohepatitis or whole-body insulin resistance despite the profound steatosis and impaired hepatic insulin signal transduction. Indeed, under the metabolic stress of a HFD, L-JAK2 KO mice exhibited enhanced glucose-stimulated insulin secretion and increased β-cell mass, leading to improved glucose tolerance compared with their control littermates.

Insulin resistance is a common finding in patients with fatty liver and animal models of NAFLD (26–28), but the causal relationship between hepatic steatosis and insulin resistance is unclear. Hyperinsulinemia resulting from systemic insulin resistance can activate the transcription of genes regulating FA synthesis and TG esterification through sterol regulatory element-binding protein 1c (SREBP-1c) (29). Alternatively, others have proposed that accumulation of bioactive lipid metabolites such as FFA, DAG, and ceramide can negatively regulate hepatic insulin signaling (30–32). On the other hand, recent data suggest that steatosis and insulin resistance may be two separate manifestations of the metabolic disturbances in response to nutritional overload (33). Specifically, an increase in circulating pro-inflammatory adipokines such as TNF-α, IL-6, and resistin in the context of visceral obesity leads to activation of inflammatory pathways that impair insulin signal transduction in the liver (34). Here we show that impairment in hepatic insulin signaling mediated by *jak2* deletion, possibly as a consequence of accumulation of fatty acid metabolites, can occur independently of changes in whole-body insulin sensitivity and in the absence of hepatic and systemic inflammation.

Despite the presence of profound fatty liver and dysregulated hepatic glucose production, L-JAK2 KO mice showed a remarkable protection against HFD-induced glucose tolerance. This metabolically beneficial profile was also apparent in chow-fed animals and could be due to several reasons. First, elevated levels of circulating leptin in L-JAK2 KO mice may improve their metabolic profile by central regulation of energy homeostasis (35). Consistent with the role of leptin in the control of energy balance, L-JAK2 KO mice displayed elevated energy expenditure compared with control littermates. Alternatively, the feedback increase in circulating GH concentration in L-JAK2 KO mice may also favor an increase in basal metabolic rate. Several lines of evidence suggest that high concentrations of GH stimulate resting energy expenditure independent of changes in lean body mass (36, 37), although the underlying mechanisms are not fully elucidated.

The protection against diet-induced glucose intolerance, on the other hand, may be explained by the compensatory increase in β-cell mass and the enhancement in glucose-stimulated insulin secretion in response to blunted insulin signaling in the liver in L-JAK2 KO mice. The effects of impaired hepatic insulin signaling on β cell mass have been well documented. For instance, hepatocyte-specific deletion of the insulin receptor has be shown to lead to β cell hyperplasia and hyperinsulinemia (38). In this model, IGF-1 was thought to act as a liver-derived growth factor to drive compensatory β cell hyperplasia through insulin receptor A isoform (39). Alternatively, hepatic activation of ERK signaling, which is enhanced in the setting of obesity-induced insulin resistance, has been proposed to stimulate β cell proliferation through a neuronal-mediated relay of metabolic signals to the pancreas (40). In addition to impaired hepatic insulin signaling, our L-JAK2 KO mice display impaired hepatic GH signaling and a significant reduction in IGF-1 production, leading to a compensatory increase in circulating GH levels. GH signaling in β cells has recently been shown to be required for glucose-stimulated insulin secretion and compensatory β cell proliferation under the stress of a HFD (41). Therefore, attenuated hepatic insulin signaling together with increased GH may contribute to the β-cell proliferation observed in L-JAK2 KO mice.

Hepatocyte-specific deletion of the leptin receptor, GH receptor, STAT3 and STAT5 all led to varying degrees of lipid deposition in the liver (12, 13, 15, 16, 18). However, whether lipid over-accumulation predisposed the knock-out mice to development of steatohepatitis was unknown. By far the most profound steatosis among all mouse models is observed with deletion of hepatic *jak2*. We are the first to show that, despite the profound steatosis, abolishment of signaling through hepatic JAK2 arrests the inflammatory progression of fatty liver. Furthermore, in contrast to our mouse model, both hepatic STAT5 (16) and GH receptor (15) knock-out mice developed glucose intolerance and whole-body insulin resistance. Hepatocyte-specific deletion of the intracellular signaling domain of the leptin receptor, on the other hand, improved hepatic insulin sensitivity the knock-out mice, resulting in protection against age- and diet-related glucose intolerance (12). Phenotypic differences in these mouse models could be attributed to impact of *jak2* deletion on multiple other signaling pathways such as the IL-6 pathway. A recent study by Sos *et al.* (19) also examined the role of JAK2 in hepatic lipid metabolism. Using the same Cre-mediated recombination driven by the albumin promoter, the investigators demonstrated that deletion of *jak2* in hepatocytes led to spontaneous steatosis, and this was dependent on excess GH signaling in peripheral tissues such that abolishment of aberrant GH secretion completely rescued the fatty liver phenotype. While we also found disrupted hepatic GH signaling and a reduction in subcutaneous and visceral adipose tissue depot in our L-JAK2 KO mice, the feedback increase in circulating GH levels was not associated with an expected decline in insulin sensitivity and glucose tol-

FIGURE 6. **L-JAK2 KO mice display a reduction in adiposity and an increase in energy expenditure.** *A*, body weight, body length measured from snout to anus, and body mass index at 1 ($n = 6–16$ per group) and 6 ($n = 6–13$ per group) months of age. *B*, visceral (perigonadal depot), subcutaneous (inguinal depot) and brown fat pads were harvested from 1- and 6-month-old mice and weighed ($n = 7–10$ per group). Results are expressed relative to total body weight. *vis.*, visceral; *s.c.*, subcutaneous. *C*, serum total FFA at 4 months of age ($n \geq 3$ per group). *D*, serum levels of individual fatty acid species ($n = 3$ per group). *E* and *F*, serum levels of (*E*) adiponectin and (*F*) leptin from mice at 1 and 4 months of age ($n \geq 5$ per group). *G–J*, chow-fed mice at 5–6 months of age were housed individually in metabolic chambers with free access to food and water and energy balance data were collected for 24 h ($n = 9$). *G*, RER, calculated as VCO_2/VO_2; *H*, oxygen consumption (VO_2) and carbon dioxide production (VCO_2); (*I*) daily food intake was determined by weighing the chow before and after the 24-h measurement. Results are expressed relative to total body weight; (*J*) physical activity, expressed as average number of infra-red beam breaks during one measurement interval. *K*, rectal temperature of chow-fed mice at 5–6 months of age measured at 10:00 AM. Results are mean ± S.E. *, $p < 0.05$; **, $p < 0.01$; ***, $p < 0.001$.

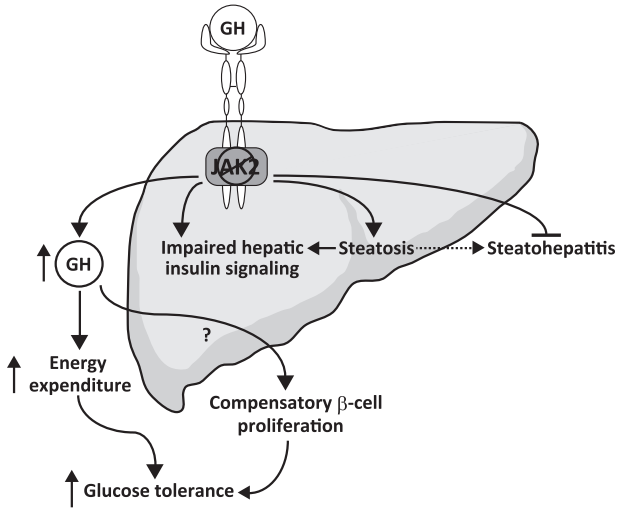

FIGURE 7. **Proposed model of the mechanism for the observed phenotype in L-JAK2 KO mice.** Deletion of JAK2 specifically in hepatocytes attenuates hepatic GH signaling, leading to lipid over-accumulation in the liver as a result of increased uptake of circulating free fatty acids. Impaired hepatic insulin signaling triggers compensatory β-cell proliferation in the pancreatic islets, leading to increased β-cell mass. Elevated GH levels may also promote compensatory β-cell proliferation in response to HFD, thereby protecting against HFD-induced glucose intolerance. Furthermore, GH may stimulate resting energy expenditure, leading to an improved metabolic profile compared with their control littermates. On the other hand, as an essential mediator of inflammatory signaling, deletion of JAK2 arrests the progression of steatosis to steatohepatitis.

erance. Indeed, L-JAK2 KO mice were more glucose tolerant than their control littermates. The phenotypic disparities between our mouse model and the one by Sos *et al.* (19) may be partly due to inherent strain differences.

Similar to the previous study, expression analysis of genes regulating hepatic lipid metabolism showed no deficiency in lipoprotein synthesis, VLDL export or FA β-oxidation (supplemental Fig. S3, *A* and *B*). There was also no abnormality in *de novo* lipogenesis (supplemental Fig. S3, *C* and *D*). On the other hand, there was a 4-fold elevation in expression of fatty acid translocase (*cd36*) in livers of L-JAK2 KO mice (supplemental Fig. S3*A*), indicating that the major contributor to lipid overstorage was increased uptake of circulating FFA. This elevation in *cd36* transcript levels was seen in all mouse models of disrupted hepatic GH signaling (15, 16, 18). Indeed, *cd36* transcription can be regulated directly by STAT5 (18, 42), or indirectly by PPARγ, whose expression is repressed by STAT5-mediated GH signaling (43, 44).

In summary, our study highlights the multiple roles of hepatic JAK2 in the regulation of lipid and carbohydrate metabolism and inflammation. Mice lacking JAK2 in hepatocytes presented with profound, spontaneous hepatic steatosis associated with attenuated insulin-stimulated phosphorylation of Akt in the liver; however, this overwhelming lipid accumulation did not progress to steatohepatitis or whole-body insulin resistance on a HFD. In fact, the feedback increase in serum GH concentration as a consequence of disrupted hepatic GH signaling likely induced the increase in resting energy expenditure, contributing to the improved metabolic profile observed in chow-fed L-JAK2 KO mice. Furthermore, both increased GH signaling and dampened hepatic insulin signaling might mediate compensatory β cell proliferation in response to HFD feeding, rendering L-JAK2 KO mice resistant to development of diet-induced glucose intolerance (Fig. 7). Taken together, our study provides new insights into the pathogenic mechanisms underlying diet-induced insulin resistance and glucose intolerance. Further understanding of the role of hepatic JAK2 in fuel metabolism and inflammation will facilitate development of novel treatment strategies for many diseases that are associated with the metabolic syndrome.

REFERENCES

1. Angulo, P. (2002) Nonalcoholic fatty liver disease. *N. Engl. J. Med.* **346,** 1221–1231
2. Szczepaniak, L. S., Nurenberg, P., Leonard, D., Browning, J. D., Reingold, J. S., Grundy, S., Hobbs, H. H., and Dobbins, R. L. (2005) Magnetic resonance spectroscopy to measure hepatic triglyceride content: prevalence of hepatic steatosis in the general population. *Am. J. Physiol. Endocrinol. Metab.* **288,** E462–468
3. Marchesini, G., Brizi, M., Bianchi, G., Tomassetti, S., Bugianesi, E., Lenzi, M., McCullough, A. J., Natale, S., Forlani, G., and Melchionda, N. (2001) Nonalcoholic fatty liver disease: a feature of the metabolic syndrome. *Diabetes* **50,** 1844–1850
4. Matteoni, C. A., Younossi, Z. M., Gramlich, T., Boparai, N., Liu, Y. C., and McCullough, A. J. (1999) Nonalcoholic fatty liver disease: a spectrum of clinical and pathological severity. *Gastroenterology* **116,** 1413–1419
5. Younossi, Z. M., Gramlich, T., Liu, Y. C., Matteoni, C., Petrelli, M., Goldblum, J., Rybicki, L., and McCullough, A. J. (1998) Nonalcoholic fatty liver disease: assessment of variability in pathologic interpretations. *Mod. Pathol.* **11,** 560–565
6. Day, C. P., and James, O. F. (1998) Steatohepatitis: a tale of two "hits"? *Gastroenterology* **114,** 842–845
7. Yamaguchi, K., Yang, L., McCall, S., Huang, J., Yu, X. X., Pandey, S. K., Bhanot, S., Monia, B. P., Li, Y. X., and Diehl, A. M. (2007) Inhibiting triglyceride synthesis improves hepatic steatosis but exacerbates liver damage and fibrosis in obese mice with nonalcoholic steatohepatitis. *Hepatology* **45,** 1366–1374
8. Matsuzawa, N., Takamura, T., Kurita, S., Misu, H., Ota, T., Ando, H., Yokoyama, M., Honda, M., Zen, Y., Nakanuma, Y., Miyamoto, K., and Kaneko, S. (2007) Lipid-induced oxidative stress causes steatohepatitis in mice fed an atherogenic diet. *Hepatology* **46,** 1392–1403
9. Shiri-Sverdlov, R., Wouters, K., van Gorp, P. J., Gijbels, M. J., Noel, B., Buffat, L., Staels, B., Maeda, N., van Bilsen, M., and Hofker, M. H. (2006) Early diet-induced non-alcoholic steatohepatitis in APOE2 knock-in mice and its prevention by fibrates. *J. Hepatol* **44,** 732–741
10. Monetti, M., Levin, M. C., Watt, M. J., Sajan, M. P., Marmor, S., Hubbard, B. K., Stevens, R. D., Bain, J. R., Newgard, C. B., Farese, R. V., Sr., Hevener, A. L., and Farese, R. V., Jr. (2007) Dissociation of hepatic steatosis and insulin resistance in mice overexpressing DGAT in the liver. *Cell Metab* **6,** 69–78
11. Gao, B. (2005) Cytokines, STATs and liver disease. *Cell Mol. Immunol.* **2,** 92–100
12. Huynh, F. K., Levi, J., Denroche, H. C., Gray, S. L., Voshol, P. J., Neumann, U. H., Speck, M., Chua, S. C., Covey, S. D., and Kieffer, T. J. (2010) Disruption of hepatic leptin signaling protects mice from age- and diet-related glucose intolerance. *Diabetes* **59,** 3032–3040
13. Inoue, H., Ogawa, W., Ozaki, M., Haga, S., Matsumoto, M., Furukawa, K., Hashimoto, N., Kido, Y., Mori, T., Sakaue, H., Teshigawara, K., Jin, S., Iguchi, H., Hiramatsu, R., LeRoith, D., Takeda, K., Akira, S., and Kasuga, M. (2004) Role of STAT-3 in regulation of hepatic gluconeogenic genes and carbohydrate metabolism *in vivo*. *Nat. Med.* **10,** 168–174
14. Vijayakumar, A., Novosyadlyy, R., Wu, Y., Yakar, S., and LeRoith, D. (2010) Biological effects of growth hormone on carbohydrate and lipid metabolism. *Growth Horm. IGF Res.* **20,** 1–7
15. Fan, Y., Menon, R. K., Cohen, P., Hwang, D., Clemens, T., DiGirolamo, D. J., Kopchick, J. J., Le Roith, D., Trucco, M., and Sperling, M. A. (2009) Liver-specific deletion of the growth hormone receptor reveals essential

role of growth hormone signaling in hepatic lipid metabolism. *J. Biol. Chem.* **284,** 19937–19944
16. Cui, Y., Hosui, A., Sun, R., Shen, K., Gavrilova, O., Chen, W., Cam, M. C., Gao, B., Robinson, G. W., and Hennighausen, L. (2007) Loss of signal transducer and activator of transcription 5 leads to hepatosteatosis and impaired liver regeneration. *Hepatology* **46,** 504–513
17. Yakar, S., Setser, J., Zhao, H., Stannard, B., Haluzik, M., Glatt, V., Bouxsein, M. L., Kopchick, J. J., and LeRoith, D. (2004) Inhibition of growth hormone action improves insulin sensitivity in liver IGF-1-deficient mice. *J. Clin. Invest.* **113,** 96–105
18. Barclay, J. L., Nelson, C. N., Ishikawa, M., Murray, L. A., Kerr, L. M., McPhee, T. R., Powell, E. E., and Waters, M. J. (2011) GH-dependent STAT5 signaling plays an important role in hepatic lipid metabolism. *Endocrinology* **152,** 181–192
19. Sos, B. C., Harris, C., Nordstrom, S. M., Tran, J. L., Balázs, M., Caplazi, P., Febbraio, M., Applegate, M. A., Wagner, K. U., and Weiss, E. J. (2011) Abrogation of growth hormone secretion rescues fatty liver in mice with hepatocyte-specific deletion of JAK2. *J. Clin. Invest.* **121,** 1412–1423
20. Iyer, A., Fairlie, D. P., Prins, J. B., Hammock, B. D., and Brown, L. (2010) Inflammatory lipid mediators in adipocyte function and obesity. *Nat. Rev. Endocrinol.* **6,** 71–82
21. Krempler, A., Qi, Y., Triplett, A. A., Zhu, J., Rui, H., and Wagner, K. U. (2004) Generation of a conditional knockout allele for the Janus kinase 2 (Jak2) gene in mice. *Genesis* **40,** 52–57
22. Wang, L., Liu, Y., Yan Lu, S., Nguyen, K. T., Schroer, S. A., Suzuki, A., Mak, T. W., Gaisano, H., and Woo, M. (2010) Deletion of Pten in pancreatic ß-cells protects against deficient ß-cell mass and function in mouse models of type 2 diabetes. *Diabetes* **59,** 3117–3126
23. Duez, H., Smith, A. C., Xiao, C., Giacca, A., Szeto, L., Drucker, D. J., and Lewis, G. F. (2009) Acute dipeptidyl peptidase-4 inhibition rapidly enhances insulin-mediated suppression of endogenous glucose production in mice. *Endocrinology* **150,** 56–62
24. Chen, C. T., Ma, D. W., Kim, J. H., Mount, H. T., and Bazinet, R. P. (2008) The low density lipoprotein receptor is not necessary for maintaining mouse brain polyunsaturated fatty acid concentrations. *J. Lipid Res.* **49,** 147–152
25. Schiffmann, S., Sandner, J., Schmidt, R., Birod, K., Wobst, I., Schmidt, H., Angioni, C., Geisslinger, G., and Grösch, S. (2009) The selective COX-2 inhibitor celecoxib modulates sphingolipid synthesis. *J. Lipid Res.* **50,** 32–40
26. Farrell, G. C., and Larter, C. Z. (2006) Nonalcoholic fatty liver disease: from steatosis to cirrhosis. *Hepatology* **43,** S99-S112
27. Marchesini, G., Brizi, M., Morselli-Labate, A. M., Bianchi, G., Bugianesi, E., McCullough, A. J., Forlani, G., and Melchionda, N. (1999) Association of nonalcoholic fatty liver disease with insulin resistance. *Am. J. Med.* **107,** 450–455
28. Seppälä-Lindroos, A., Vehkavaara, S., Häkkinen, A. M., Goto, T., Westerbacka, J., Sovijärvi, A., Halavaara, J., and Yki-Järvinen, H. (2002) Fat accumulation in the liver is associated with defects in insulin suppression of glucose production and serum free fatty acids independent of obesity in normal men. *J. Clin. Endocrinol. Metab.* **87,** 3023–3028
29. Matsumoto, M., Ogawa, W., Akimoto, K., Inoue, H., Miyake, K., Furukawa, K., Hayashi, Y., Iguchi, H., Matsuki, Y., Hiramatsu, R., Shimano, H., Yamada, N., Ohno, S., Kasuga, M., and Noda, T. (2003) PKClambda in liver mediates insulin-induced SREBP-1c expression and determines both hepatic lipid content and overall insulin sensitivity. *J. Clin. Invest.* **112,** 935–944
30. Kim, J. K., Fillmore, J. J., Chen, Y., Yu, C., Moore, I. K., Pypaert, M., Lutz, E. P., Kako, Y., Velez-Carrasco, W., Goldberg, I. J., Breslow, J. L., and Shulman, G. I. (2001) Tissue-specific overexpression of lipoprotein lipase causes tissue-specific insulin resistance. *Proc. Natl. Acad. Sci. U.S.A.* **98,** 7522–7527
31. Ruddock, M. W., Stein, A., Landaker, E., Park, J., Cooksey, R. C., McClain, D., and Patti, M. E. (2008) Saturated fatty acids inhibit hepatic insulin action by modulating insulin receptor expression and post-receptor signalling. *J. Biochem.* **144,** 599–607
32. Ussher, J. R., Koves, T. R., Cadete, V. J., Zhang, L., Jaswal, J. S., Swyrd, S. J., Lopaschuk, D. G., Proctor, S. D., Keung, W., Muoio, D. M., and Lopaschuk, G. D. (2010) Inhibition of de novo ceramide synthesis reverses diet-induced insulin resistance and enhances whole-body oxygen consumption. *Diabetes* **59,** 2453–2464
33. Arkan, M. C., Hevener, A. L., Greten, F. R., Maeda, S., Li, Z. W., Long, J. M., Wynshaw-Boris, A., Poli, G., Olefsky, J., and Karin, M. (2005) IKK-β links inflammation to obesity-induced insulin resistance. *Nat. Med.* **11,** 191–198
34. Shoelson, S. E., Lee, J., and Goldfine, A. B. (2006) Inflammation and insulin resistance. *J. Clin. Invest.* **116,** 1793–1801
35. Gautron, L., and Elmquist, J. K. (2011) Sixteen years and counting: an update on leptin in energy balance. *J. Clin. Invest.* **121,** 2087–2093
36. Bray, G. A. (1969) Calorigenic effect of human growth hormone in obesity. *J. Clin. Endocrinol. Metab.* **29,** 119–122
37. Wolthers, T., Grøftne, T., Møller, N., Christiansen, J. S., Orskov, H., Weeke, J., and Jørgensen, J. O. (1996) Calorigenic effects of growth hormone: the role of thyroid hormones. *J. Clin. Endocrinol. Metab.* **81,** 1416–1419
38. Michael, M. D., Kulkarni, R. N., Postic, C., Previs, S. F., Shulman, G. I., Magnuson, M. A., and Kahn, C. R. (2000) Loss of insulin signaling in hepatocytes leads to severe insulin resistance and progressive hepatic dysfunction. *Mol. Cell* **6,** 87–97
39. Escribano, O., Guillén, C., Nevado, C., Gómez-Hernandez, A., Kahn, C. R., and Benito, M. (2009) Beta-Cell hyperplasia induced by hepatic insulin resistance: role of a liver-pancreas endocrine axis through insulin receptor A isoform. *Diabetes* **58,** 820–828
40. Imai, J., Katagiri, H., Yamada, T., Ishigaki, Y., Suzuki, T., Kudo, H., Uno, K., Hasegawa, Y., Gao, J., Kaneko, K., Ishihara, H., Niijima, A., Nakazato, M., Asano, T., Minokoshi, Y., and Oka, Y. (2008) Regulation of pancreatic beta cell mass by neuronal signals from the liver. *Science* **322,** 1250–1254
41. Wu, Y., Liu, C., Sun, H., Vijayakumar, A., Giglou, P. R., Qiao, R., Oppenheimer, J., Yakar, S., and LeRoith, D. (2011) Growth hormone receptor regulates β cell hyperplasia and glucose-stimulated insulin secretion in obese mice. *J. Clin. Invest.* **121,** 2422–2426
42. Cheung, L., Andersen, M., Gustavsson, C., Odeberg, J., Fernández-Pérez, L., Norstedt, G., and Tollet-Egnell, P. (2007) Hormonal and nutritional regulation of alternative CD36 transcripts in rat liver-a role for growth hormone in alternative exon usage. *BMC Mol. Biol.* **8,** 60
43. Chawla, A., Barak, Y., Nagy, L., Liao, D., Tontonoz, P., and Evans, R. M. (2001) PPAR-γ-dependent and independent effects on macrophage-gene expression in lipid metabolism and inflammation. *Nat. Med.* **7,** 48–52
44. Zhou, Y. C., and Waxman, D. J. (1999) Cross-talk between janus kinase-signal transducer and activator of transcription (JAK-STAT) and peroxisome proliferator-activated receptor-α (PPARα) signaling pathways. Growth hormone inhibition of PPARα transcriptional activity mediated by stat5b. *J. Biol. Chem.* **274,** 2672–2681